

Numerical measurements of the shape and dispersion relation for moving one-dimensional anharmonic localized modes

S. R. Bickham and A. J. Sievers

Laboratory of Atomic and Solid State Physics and Materials Science Center, Cornell University, Ithaca, New York 14853-2501

S. Takeno

Department of Physics, Faculty of Engineering and Design, Kyoto Institute of Technology, Kyoto, Japan

(Received 26 November 1991)

Computer simulations show that in a one-dimensional lattice both even and odd anharmonic localized modes can move with constant velocity. For nearest-neighbor forces described by a harmonic plus hard quartic potential, the dispersion relation $\omega(k)$ has been calculated for both types of modes. Numerical experiments show that, in general, moving modes with a near-Gaussian excitation envelope occur in parts of $\omega(k)$ space, with this region becoming more restricted as the local-mode frequency increases.

Recent studies with analytical¹⁻⁴ and simulation⁵⁻⁷ methods on the dynamical properties of perfect lattices with quadratic and hard quartic anharmonicity have shown the existence of stationary localized modes above the top of the harmonic frequency band of a pure crystal lattice. The characteristic feature of the stationary anharmonic localized mode is that it can appear in a lattice of any dimensionality,^{3,7,8} provided that the condition for its existence is satisfied. Simulations of moving even localized modes have been mentioned briefly in the literature.^{5,6,9} Using the continuum approximation, which cannot be extended to two and three dimensions, Burlakov *et al.*¹⁰ presented a few preliminary numerical experiments.

In this paper, the dispersion curve for moving even and odd anharmonic localized modes in a one-dimensional (1D) lattice is explored with simulations and detailed numerical tests. The results are that for both types of modes uniform translational motion can be produced over part of $\omega(k)$ space with the k range becoming more restricted as the local-mode frequency is increased. A Gaussian-like envelope function provides a good fit to the simulated vibrational soliton. When such an analytical form is used to characterize the motion, the vibrational frequency, wave vector, and group velocity can be identified.

A perfect 1D crystal lattice is considered in which each particle with mass m interacts only with its nearest neighbors with the harmonic force constant K_2 and the anharmonic constant K_4 derived from the positive quartic anharmonic potential. The equation of motion for the displacement u_n of the n th atom from its equilibrium position is¹¹

$$m \frac{d^2 u_n}{dt^2} = K_2(u_{n+1} + u_{n-1} - 2u_n) + K_4[(u_{n+1} - u_n)^3 - (u_n - u_{n-1})^3]. \quad (1)$$

To describe the properties of an even localized mode of the type shown at the top of Fig. 1(a), it is helpful to change to a different lattice by the transformation

$$w_n = u_{n+1} - u_n, \quad (2)$$

so that the symmetry type is changed to an odd mode using this transformed displacement-field variable, as shown at the bottom of Fig. 1(a). Equation (1) now be-

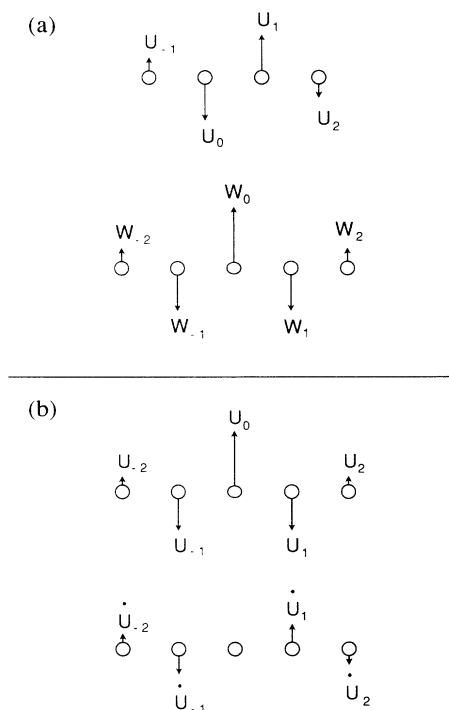


FIG. 1. Initial conditions for the generation of moving modes. (a) Top: Initial longitudinal displacements for an even mode in u space. Bottom: the corresponding odd mode in w space. The vectors are drawn in the transverse direction for clarity. These two spaces are related by Eq. (2) in the text. (b) Top: Initial longitudinal displacements for an odd mode in u space. Bottom: Initial velocities for an odd mode in u space. Again, transverse vectors are used for clarity. The wave vector for this moving excitation is $ka = 0.1$ and the anharmonicity parameter $\Lambda = 0.9$, so that $\omega/\omega_m = 1.48$, where ω_m is the maximum frequency of the harmonic plane-wave spectrum.

comes⁹

$$\frac{d^2 w_n}{dt^2} = J_2(w_{n+1} + w_{n-1} - 2w_n) + J_4(w_{n+1}^3 + w_{n-1}^3 - 2w_n^3), \quad (3)$$

where $J_2 = K_2/m$ and $J_4 = K_4/m$. The maximum frequency of the plane-wave spectrum is $\omega_m^2 = 4J_2$ since the anharmonic terms are negligible for the small amplitude limit appropriate to a plane-wave spectrum.¹

An analytic solution to Eq. (3), giving a moving anharmonic mode, is sought by setting

$$w_n = \alpha \phi_n(t) \cos(kna + \omega t), \quad (4)$$

where α is the maximum amplitude of the moving localized mode in a lattice with spacing a , $\phi_n(t)$ is an envelope function, $\cos(kna + \omega t)$ is a left-moving carrier wave function, and k and ω are the wave vector and frequency, respectively, of the carrier wave describing the localized mode. Inserting Eq. (4) into Eq. (3) and using the rotating-wave approximation (RWA),¹ we get a pair of equations. Equating the sine terms gives⁹

$$\frac{d\phi_n}{dt} = v_k(\phi_{n+1} - \phi_{n-1}) \times [1 + (3\Lambda/4)(\phi_{n+1}^2 + \phi_{n+1}\phi_{n-1} + \phi_{n-1}^2)], \quad (5)$$

and the cosine terms,

$$\omega^2 \phi_n - \frac{d^2 \phi_n}{dt^2} = J_2 \{ [2\phi_n - (\phi_{n+1} + \phi_{n-1}) \cos(ka)] + (3\Lambda/4) [2\phi_n^3 - (\phi_{n+1}^3 + \phi_{n-1}^3) \cos(ka)] \}, \quad (6)$$

where $v_k = (J_2/2\omega) \sin(ka)$ and $\Lambda = J_4 \alpha^2 / J_2 = K_4 \alpha^2 / K_2$. We assume that the time variation of the envelope function is small compared with that of the carrier wave, i.e., $\omega^2 \phi_n \gg d^2 \phi_n / dt^2$; then¹²

$$(\omega/\omega_m)^2 \phi_n = \frac{1}{4} \{ [2\phi_n - (\phi_{n+1} + \phi_{n-1}) \cos(ka)] + (3\Lambda/4) [2\phi_n^3 - (\phi_{n+1}^3 + \phi_{n-1}^3) \cos(ka)] \}. \quad (7)$$

This set of time-independent equations can be used to identify the initial displacement pattern of the mode, and then Eq. (5) can be used to find the initial velocity pattern. Note that for $k=0$, Eq. (7) reduces to the previously determined eigenvalue equation, giving the eigenfrequency and eigenfunction of the stationary even mode.^{4,7,8,13}

To find the corresponding displacements and velocities for the odd mode with a particular wave vector, shown in Fig. 1(b), it is easier to work directly in u space. Assuming a form of the solution similar to Eq. (4), the differential equation corresponding to Eq. (5) is

$$\frac{d\phi_n}{dt} = v_k(\phi_{n+1} - \phi_{n-1}) \{ 1 + (3\Lambda/4) [\phi_{n+1}^2 + \phi_{n+1}\phi_{n-1} + \phi_{n-1}^2 + \phi_n^2 - 2(\phi_{n+1} + \phi_{n-1})\phi_n \cos(ka)] \}. \quad (8)$$

Once again, for relatively slow time variation of the envelope function, the analog of Eq. (7) is

$$\left[\frac{\omega}{\omega_m} \right]^2 \phi_n = \frac{1}{4} \left\{ 2\phi_n - (\phi_{n+1} + \phi_{n-1}) \cos(ka) + \frac{3\Lambda}{4} \{ 2\phi_n^3 - (\phi_{n+1}^3 + \phi_{n-1}^3) \cos(ka) + (\phi_{n+1}^2 + \phi_{n-1}^2) \phi_n [1 + 2 \cos^2(ka)] - 3(\phi_{n+1} + \phi_{n-1}) \phi_n^2 \cos(ka) \} \right\}. \quad (9)$$

These two sets of equations [Eqs. (5) and (7) or (8) and (9)] determine the initial amplitudes and velocities necessary to produce a localized mode with frequency ω and wave vector k . To truncate the series of equations in either w or u space, we assume that the mode is localized and introduce the following trial solution for $t=0$:

$$\phi_0 = \alpha, \quad \phi_n = \phi_{-n}, \quad \phi_n = (-1)^{|n|} \alpha A e^{-nKa}, \quad (10)$$

for K positive.⁷ For a given value of k and Λ , the time-independent equations for sites $n=0, 1, 2$ are numerically solved for $\omega(k)/\omega_m$, A , and K . Hence $\omega(k)$ is found and the latter two quantities give the initial amplitudes. When all three quantities are substituted into either Eq. (5) or (8), the initial velocities are determined. These values are used as initial conditions for the moving

even and odd modes in the simulations.

To determine if these modes actually do move, we numerically integrate the equations of motion [either Eq. (3) or (1)] using a fifth-order Gear predictor-corrector algorithm¹⁴ for a chain of 100 particles with periodic-boundary conditions. A small time step $\Delta t = 1/(200\omega_m)$ is used in order to approximately conserve energy over the time interval of the measurement.

Figure 2 presents the trajectory of the moving odd localized mode produced with the same initial amplitudes and velocities as given in Fig. 1(b). Plots of the displacement versus time at three different sites are overlaid to illustrate how the particle responds as the excitation passes and also to demonstrate that the velocity of the excitation packet is a constant. The farthest that we have tracked

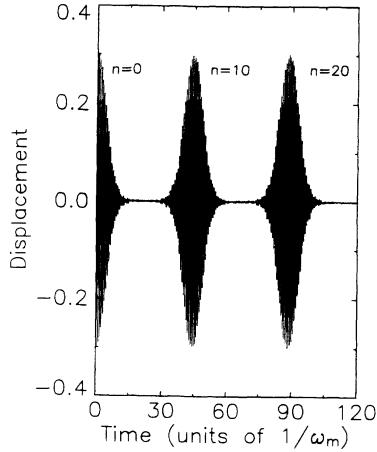


FIG. 2. Excitation passing three different lattice sites as a function of times. The displacement amplitude of the particle at $n=0$ decreases with increasing time. Superimposed on top of that picture are the increasing and decreasing amplitudes at sites $n=10$ and 20 as the vibrational envelope moves along the 100-atom chain. The velocity of the envelope V_g is 7.2% of the sound velocity. Here ω_m is the maximum frequency of the harmonic plane-wave spectrum.

this particular moving mode with parameter values given in Fig. 1(b) is 400 lattice sites, which corresponds to a time of 1800 periods of ω_m . The ripples in the figure between the packets represent plane waves that are excited when the initial conditions do not correspond to the exact eigenfunction of the moving mode. The relatively small amplitudes seen here attest to the accuracy of these particular initial conditions.

The calculated dispersion curves for the even mode for four different anharmonicity values are given by the dashed lines in Fig. 3. In each case the solid line

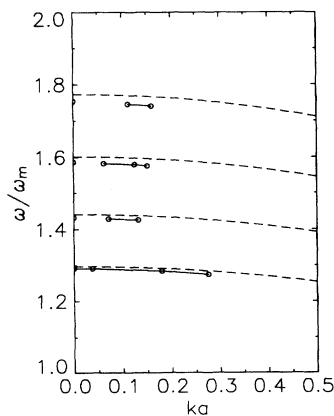


FIG. 3. Dispersion curve of the even mode in u space for four different anharmonicity values. The values from top to bottom are $\Lambda=4.9, 3.6, 2.5,$ and 1.6 . The dashed lines identify solutions of the equations of motion using the localization condition given by Eq. (10) in the text. The solid lines indicate regions where simulations of moving modes are successful. The open circles are determined from the simulated displacements by assuming that a Gaussian function [see Eq. (11)] describes the excitation envelope.

identifies the region of $\omega(k)$ space where the excitation moves with a constant envelope velocity over at least 15 lattice sites. This velocity is typically smaller than 15% of the lattice sound velocity. The absence of a solid line at small k values identifies that region where the mode either does not move or moves only a few sites and then stops. At larger k values, on the other side of the solid line, the mode moves, but decelerates. Figure 4 presents qualitatively similar results for the odd mode for four different anharmonicity values, but now uniform motion is observed over a larger region of $\omega(k)$ space than is found for the even mode in Fig. 3.

Another approach that we have used to characterize the moving excitation packet is to assume, on the basis of shape shown in Fig. 2, a specific envelope amplitude form for ϕ_n , namely,

$$w_n = (-1)^n \alpha \exp\{-[K(na - V_g t)]^2\} \cos(kna + \omega t).$$

(11)

The same prescription can be used to describe u_n . When this form is substituted directly into the equations of motion [Eqs. (5) and (7) or (8) and (9)] to obtain the initial conditions, the plane-wave ripples in the simulation data are slightly larger than when Eq. (10) is used, hence Eq. (10) is a better approximation to the initial eigenfunction than Eq. (11). Therefore we have only used Eq. (11) to fit the displacement versus time results to obtain the dispersion curve. The parameters are numerically determined from the simulation amplitudes of the excitation as it travels through four consecutive lattice sites from $n=10$ to 13.

The solid line in Fig. 5 shows a typical simulation trace of displacement versus time with a Gaussian-function best fit represented by the dashed curve. Note that a hyperbolic-secant-function best fit represented by the dotted curve does not agree with the simulated amplitude in the wings, while the Gaussian envelope matches fairly

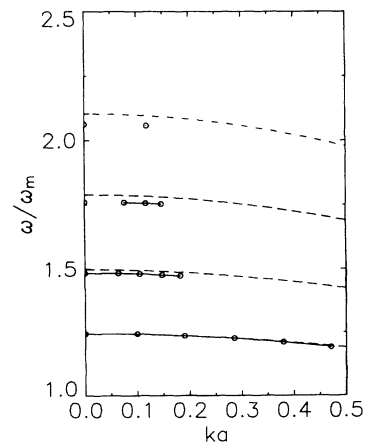


FIG. 4. Dispersion curve of the odd mode in u space for four different anharmonicity values. The values from top to bottom are $\Lambda=2.5, 1.6, 0.9,$ and 0.4 . The results are qualitatively similar to those found for the even mode described in Fig. 3, but the moving modes cover a larger area of $\omega(k)$ space.

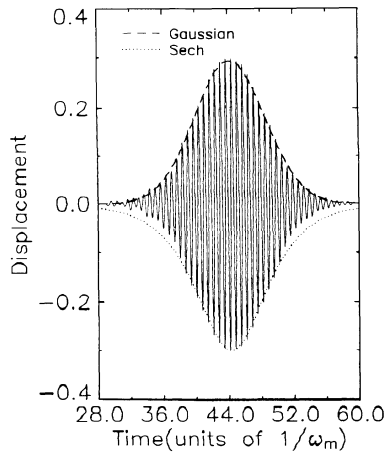


FIG. 5. Displacement vs time as the vibrational excitation passes through site 10. The solid curve gives the simulated results for the same parameter values as described in Fig. 1(b). The dashed curve represents the best fit of the excitation envelope to a Gaussian function line shape as given by Eq. (11). For comparison the dotted curve represents a hyperbolic-secant-function envelope.

well over the entire time interval.¹⁵

The resultant measured dispersion curve obtained with the specific functional form given by Eq. (11) is represented by the open circles in Figs. 3 and 4 for the even and odd modes, respectively. For the lowest-frequency modes, there is good agreement between the dashed line and open circles. Even at the largest anharmonicity value, the difference between the two curves is less than 3%, and most of this discrepancy is associated with the first-order correction⁷ to the rotating-wave approximation, missing from Eq. (5), (6), (8), and (9), and

hence the dashed curves.

The moving anharmonic localized mode in the 1D anharmonic lattice obtained from these simulations is the first systematic study of a moving vibrational soliton in a discrete lattice; the shape is different from the hyperbolic secant function previously found for continuous systems treated in plasma physics and nonlinear optics.^{16,17} Our result is also basically different from the Toda discrete lattice soliton,^{18,19} which exhibits a sech^2 envelope and contains no high-frequency oscillatory behavior, and from the soliton solution of the discrete Ablowitz-Ladik equation,²⁰ which is of the form $C \text{sech}[K(na - Vt)] \exp[i(kna - \omega t)]$. An additional important difference is that Eq. (1) is a typical nonlinear lattice-field equation in solid-state physics, while the Ablowitz-Ladik equation was originally motivated mathematically by the inverse-scattering formalism in soliton theory¹⁶ and is not derivable from a Hamiltonian. Finally, the approach used here to examine the odd vibrational modes may also be applied to two- or three-dimensional lattices; hence it may identify a way to study solitons in higher dimensions, in contrast with conventional methods¹⁶ where the general existence of solitons has only been established in one dimension.

We thank Professor R. H. Silsbee and Professor R. O. Pohl for helpful discussions. The hospitality of Professor K. Nagasaka and the Physics Department at the Science University of Tokyo where part of this manuscript was completed is gratefully acknowledged by A.J.S. The work by S.R.B. and A.J.S. has been supported by the NSF, Grant No. DMR-89-18894 and by the ARO, Grant Nos. DAAL03-K-0053 and DAAL03-90-G-0040. Computing facilities were provided in part by the Cornell-IBM Joint Study on Computing for Scientific Research. In addition, S.R.B. received partial support from AT&T Bell Laboratories.

¹A. J. Sievers and S. Takeno, *Phys. Rev. Lett.* **61**, 970 (1988).

²S. Takeno and A. J. Sievers, *Solid State Commun.* **67**, 1023 (1988).

³S. Takeno *et al.*, *Prog. Theor. Phys. Suppl.* **94**, 242 (1988).

⁴J. B. Page, *Phys. Rev. B* **41**, 7835 (1990).

⁵R. Bourbonnais and R. Maynard, *Phys. Rev. Lett.* **64**, 1397 (1990); R. Bourbonnais, Ph.D. thesis, L'Université Joseph Fourier, Grenoble, 1989.

⁶V. M. Burlakov *et al.*, *Solid State Commun.* **74**, 327 (1990); *Phys. Rev. B* **42**, 4921 (1990).

⁷S. R. Bickham and A. J. Sievers, *Phys. Rev. B* **43**, 2339 (1991).

⁸S. Takeno, *J. Phys. Soc. Jpn.* **59**, 1571 (1990).

⁹S. Takeno and J. Hori, *J. Phys. Soc. Jpn.* **59**, 3037 (1990). The approximate equations of motion introduced in this work to obtain analytically tractable results do not agree with the simulated solutions of Eq. (1) given here.

¹⁰V. M. Burlakov *et al.*, *Phys. Lett. A* **147**, 130 (1990); *Pis'ma Zh. Eksp. Teor. Fiz.* **51**, 481 (1990) [*JETP Lett.* **51**, 544 (1990)].

¹¹The first numerical simulations of plane-wave modes for this equation are described by E. Fermi, J. R. Pasta, and S. M.

Ulam, in *Collected Works of E. Fermi*, edited by E. Segrè (University of Chicago Press, Chicago, 1965), Vol. II, p. 978.

¹²Simulations, considered later in this paper, show that the $d^2\phi_n/dt^2$ is always much less than 1% of $\omega^2\phi_n$.

¹³Because of the definition of w_n , the even mode Λ in Ref. 7 is $\frac{1}{4}$ of Λ in Eq. (8).

¹⁴M. P. Allen and D. J. Tildesley, *Computer Simulation of Liquids* (Clarendon, Oxford, 1989), p. 82.

¹⁵For high frequencies where the k range is restricted, the envelope of a moving mode has a Gaussian shape, but the width is modulated by a single low frequency in the acoustic spectrum.

¹⁶See, for example, R. K. Dodd *et al.*, *Solitons and Nonlinear Wave Equations* (Academic, New York, 1988).

¹⁷W. Chen and D. L. Mills, *Phys. Rev. Lett.* **58**, 160 (1987); D. L. Mills and S. E. Trullinger, *Phys. Rev. B* **36**, 947 (1987).

¹⁸M. Toda, *J. Phys. Soc. Jpn.* **22**, 431 (1967); **23**, 501 (1967).

¹⁹M. Toda, *Theory of Nonlinear Lattices*, Vol. 20 of *Solid State Sciences* (Springer, Berlin, 1981).

²⁰M. J. Ablowitz and J. J. Ladik, *J. Math. Phys.* **17**, 1011 (1976).

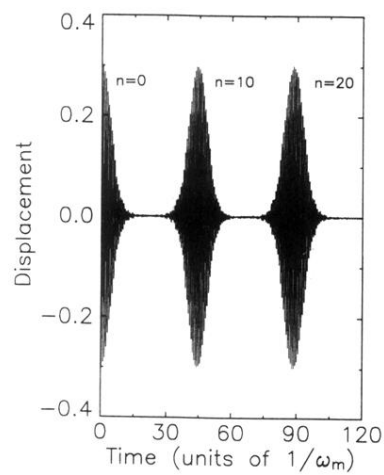


FIG. 2. Excitation passing three different lattice sites as a function of times. The displacement amplitude of the particle at $n=0$ decreases with increasing time. Superimposed on top of that picture are the increasing and decreasing amplitudes at sites $n=10$ and 20 as the vibrational envelope moves along the 100-atom chain. The velocity of the envelope V_g is 7.2% of the sound velocity. Here ω_m is the maximum frequency of the harmonic plane-wave spectrum.